

AN ABSTRACT OF THE THESIS OF

Iain Anderson _____ for the degree of _____ Master of Science
in _____ Oceanography _____ presented on _____ April 30, 1982

Title: _____ Near-Inertial Motions off the Oregon Coast _____

Abstract Approved: _____ Redacted for Privacy _____
Adriana Huyer

Nearly three months of current meter records from five moorings off the Oregon coast taken between October 1977 and January 1978 were analyzed for near-inertial motions. The moorings were located from the mid-shelf out to the foot of the continental slope, spanning the continental margin. All but two of the eleven current meters were continuously below the mixed layer. For spectral analysis, the current observation period was divided into two time periods, one with large amplitude near-inertial motion (41.1 cm/sec maximum of the band-passed records) throughout and the other with much less near-inertial energy. The spectra of the current meter records showed between a 1 and 6% increase in frequency of the near-inertial peak above f ($= 0.0592$ cph) in all but three cases. The exceptions showed spectral peaks about 14% below f and were linked to a Doppler shift. The period of large amplitude near-inertial motion had diagonal coherence scales of over 450 meters vertically and 115 kilometers horizontally. An east-west (cross-shelf) wavelength of about 50 kilometers was estimated directly from the phase differences between current meters with roughly horizontal separations.

The observed response of a current meter about 35 meters below the mixed layer to sharp maxima in the wind stress was similar to that

predicted by the Pollard and Millard (1970) model for wind forced near-inertial motions in the surface mixed layer. The winds associated with a series of atmospheric fronts were apparently responsible for generating a 14-day period of large amplitude near-inertial motion observed below the mixed layer.

NEAR-INERTIAL MOTIONS OFF THE OREGON COAST

by

Iain Anderson

A THESIS

submitted to

Oregon State University

in partial fulfillment of
the requirements for the
degree of

Master of Science

Commencement June 1982

APPROVED:

Redacted for Privacy

Associate Professor of Oceanography
in charge of major

Redacted for Privacy

Dean of the School of Oceanography

Redacted for Privacy

Dean of the Graduate School

Date Thesis is Presented: April 30, 1982

Typed by Rebecca Simpkins for: Iain Anderson

ACKNOWLEDGEMENTS

The collection and preliminary analysis of the data used in this thesis was supported by the National Science Foundation grants OCE 77-07932 and OCE 77-08791. Part of the data analyzed herein was graciously furnished by Barbara Hickey of the University of Washington. The writing and computer time necessary to complete my thesis was supported by grants from the United States Coast Guard and grant OCE 79-25019 from the National Science Foundation.

I would like to thank Joseph Bottero for the use of his bandpass filter routine. Thanks to Bill Gilbert for his assistance with the figures. The support and guidance of my major professor, Jane Huyer, was much appreciated from the initial beginnings to the finished thesis. Thanks also to Rick Romea for comments on the initial drafts of the thesis and taking time for discussion and to answer my questions.

But most of all, I would like to thank my wife, Leslie, for providing the much needed and welcomed moral support, understanding, and love necessary to complete this project.

TABLE OF CONTENTS

| | | <u>Page</u> |
|------|-------------------|-------------|
| I. | Introduction | 1 |
| II. | Data Set | 5 |
| III. | Spectral Analysis | 14 |
| IV. | Band-Passed Data | 28 |
| V. | Wind Forcing | 37 |
| VI. | Summary | 47 |
| VII. | Bibliography | 49 |

LIST OF FIGURES

| <u>Figure</u> | | <u>Page</u> |
|---------------|---|-------------|
| 1 | Location map of the moorings of the Slope Undercurrent Study and the moorings of the other near-inertial studies off Oregon. | 3 |
| 2 | Summary of the time span of the current meter data. | 7 |
| 3 | The U component of the processed data time series for all eleven current meters. | 10 |
| 4 | The Brunt-Vaisala, N^2 , profiles for the CTD cast closest to each current meter for the dates indicated. | 12 |
| 5 | The auto and cross-spectrum of Leopard 70m U and V components. | 15 |
| 6 | The power spectra of the U component of each current meter for the first and second time period. | 18 |
| 7 | The significantly coherent current meter pairs from the first and second time periods. | 24 |
| 8 | The band-pass filter and the response of the filter to synthetic time series of 5, 10, 15 cycles at 0.0625 cph. | 30 |
| 9 | The U component of the band-passed time series for all eleven current meters. | 33 |
| 10 | The U and V components of the processed and band-passed records of Leopard 70m. | 35 |
| 11 | A ten day expanded section of the band-passed U and V components of Leopard 70m from the "event" of late October/early November. | 36 |
| 12 | The Newport wind stress and the U components of the Pollard and Millard model and the Leopard 70m and Elephant 23m band-passed records. | 40 |
| 13 | The low-passed (< 0.025 cph) Newport wind direction, the Newport barometric pressure and examples of the surface synoptic charts for the period of the near-inertial "event" of late October/early November. | 44 |
| 14 | The difference in phase between the Leopard 70m, and Elephant 23m current vectors and a reference vector rotating with a frequency of 0.0625 cph. | 46 |

LIST OF TABLES

| <u>Table</u> | | <u>Page</u> |
|--------------|---|-------------|
| 1 | Values of coherence squared at the near-inertial frequencies between the U and V components of each current meter for both time periods. | 16 |
| 2 | Horizontal east-west (cross-shelf) wavelengths required to account for the phase differences between the nearly horizontally separated current meter pairs. | 25 |

NEAR-INERTIAL MOTIONS OFF THE OREGON COAST

INTRODUCTION

Near-inertial motions have been observed at all depths in the oceans and large lakes of the world (Webster, 1968). These motions are defined as circularly rotating current vectors with a period equal to about half the time required for a complete rotation of the plane in which a Foucault pendulum swings. This period depends on latitude, and the corresponding frequency is called the local inertial frequency or the Coriolis parameter, f . The rotation is clockwise in the Northern hemisphere and counter-clockwise in the Southern hemisphere. The current records examined here have a strong component which falls into this category.

The most commonly observed characteristics of near-inertial motions are well documented (Kroll, 1975; Kundu, 1976; Thomson and Huggett, 1981a). The observed frequency, ω , of near-inertial motions is generally slightly greater (3 to 20%) than the local inertial frequency, f , though there are some cases where ω was less than f (Kundu, 1976; Thomson and Huggett, 1981a; Fu, 1981). Near-inertial motions are highly intermittent and generally last only a few oscillations with a maximum velocity of 20-30 cm/sec. Vertical coherence scales of near-inertial motions are of the order of only a few tens of meters, while the horizontal coherence scale is of the order of a few tens of kilometers.

Studies of inertial currents have usually been conducted in either the open ocean (eg, Pollard, 1970, 1980; Fu, 1981) or over the continental shelf (eg, Johnson, 1976; Thomson and Huggett, 1981a). To date,

there have been three published studies of near-inertial motion off the Oregon coast. Kindle (1974) looked at horizontally separated current meters, Kundu (1976) examined vertically separated current meter records while Johnson (1976) examined both horizontally and vertically separated records. All three of these papers used data collected over the continental shelf during the summer (Figure 1).

Kindle (1974) examined the horizontal coherence of near-inertial motions over distances of 9 to 35 kilometers using current meter records of 10 to 27 days in length. The coherences found were relatively low with most being insignificant.

Kundu (1976) analyzed nearly two months of current meter data from eleven current meters at a single station. The spectrum of each record showed about an 8% increase in frequency of the near-inertial peak above f . The Pollard and Millard (1970) model of local wind forcing qualitatively reproduced many of the features of the near-inertial motion observed in the surface layer.

Johnson (1976) used 64 hours of data from a three element Cyclesonde array moored in the summer of 1972 as part of the Coastal Upwelling Experiment. A cyclesonde is a current meter that automatically cycles up and down through the water column, thus obtaining vertical profiles of the current. Johnson (1976) found the near-inertial motions were highly coherent over an 11 kilometer alongshore separation but were not coherent over a 15 kilometer cross-shelf separation.

Between October 1977 and January 1978, moored current meter measurements were made at five sites on an offshore section along 45°

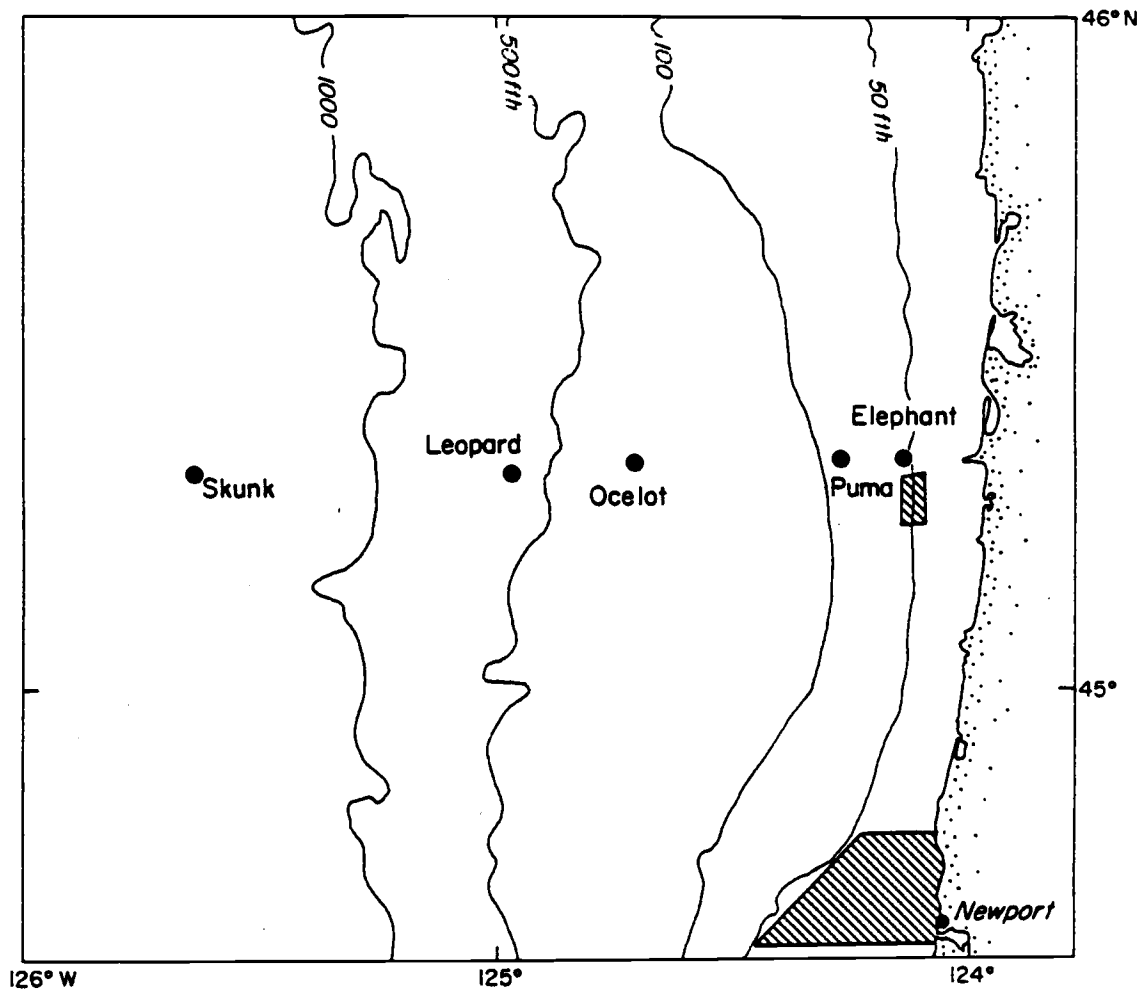


FIGURE 1

Location of the moorings of the Slope Undercurrent Study. The small shaded area is the location of the data analyzed by Kundu (1976) and the center of the array was by Johnson (1976). The large area was the location of the moorings used by Kindle (1974).

20'N spanning the continental margin off the Oregon coast (Figure 1). These measurements were part of the Slope Undercurrent Study, SUS, a joint program conducted by the University of Washington and Oregon State University. The SUS array moorings were designated Skunk, moored just seaward of the foot of the continental slope; Leopard, moored at about mid-slope; Ocelot, moored on the upper slope; Puma, moored at the shelf break; and Elephant, moored at mid-shelf. The Ocelot and Elephant moorings were maintained by the University of Washington and the remainder by Oregon State University. Although the SUS array was not originally designed to study near-inertial motions, the data provides an opportunity to examine near-inertial motions over the continental margin where no previous study has been conducted.

DATA SET

All of the SUS array moorings were sub-surface and Aanderaa current meters were used throughout. Instrument failure and losses were greater than usual for both institutions, leading to irregularly spaced current records. The Puma mooring set in October was almost immediately lost to trawling and was replaced in November. The destruction and subsequent replacement of Puma gave only a 390 hour period of simultaneous data collection from all five moorings.

Current meters that produced usable speed and direction records were: 100m, 600m, 1850m at Skunk (bottom depth 2597m); 70m, 820m at Leopard (bottom depth 1100m); 141m, 243m, 371m at Ocelot (bottom depth 600m); 64m, 164m, 261m at Puma (bottom depth 301m), and 23m, 49m, 89m at Elephant (bottom depth 110m) (Figure 2). All instruments sampled at intervals of 40 minutes. Note that no two current meters were located at the same depth in the water column.

The raw Aanderaa data records were converted to engineering units using the latest calibration equations. The total number of lines in the record was multiplied by the sampling interval and then compared against elapsed deployment time as a check of the instrument clock. Time series of speed were plotted for error detection. Spurious data points were replaced with a linear interpolation between the previous and subsequent points (Barstow, et al, 1979). After removal of obvious errors, the speed and direction were used to determine the eastward (U) and northward (V) components of the recorded currents. Record gaps of 120 hours beginning at 0900 10 October in Ocelot 371m and 136 hours beginning at 0200 9 December in Puma 261m were filled

FIGURE 2

Summary of the time span of the current meter data of the SUS array. The two time periods used for spectral analysis are indicated.

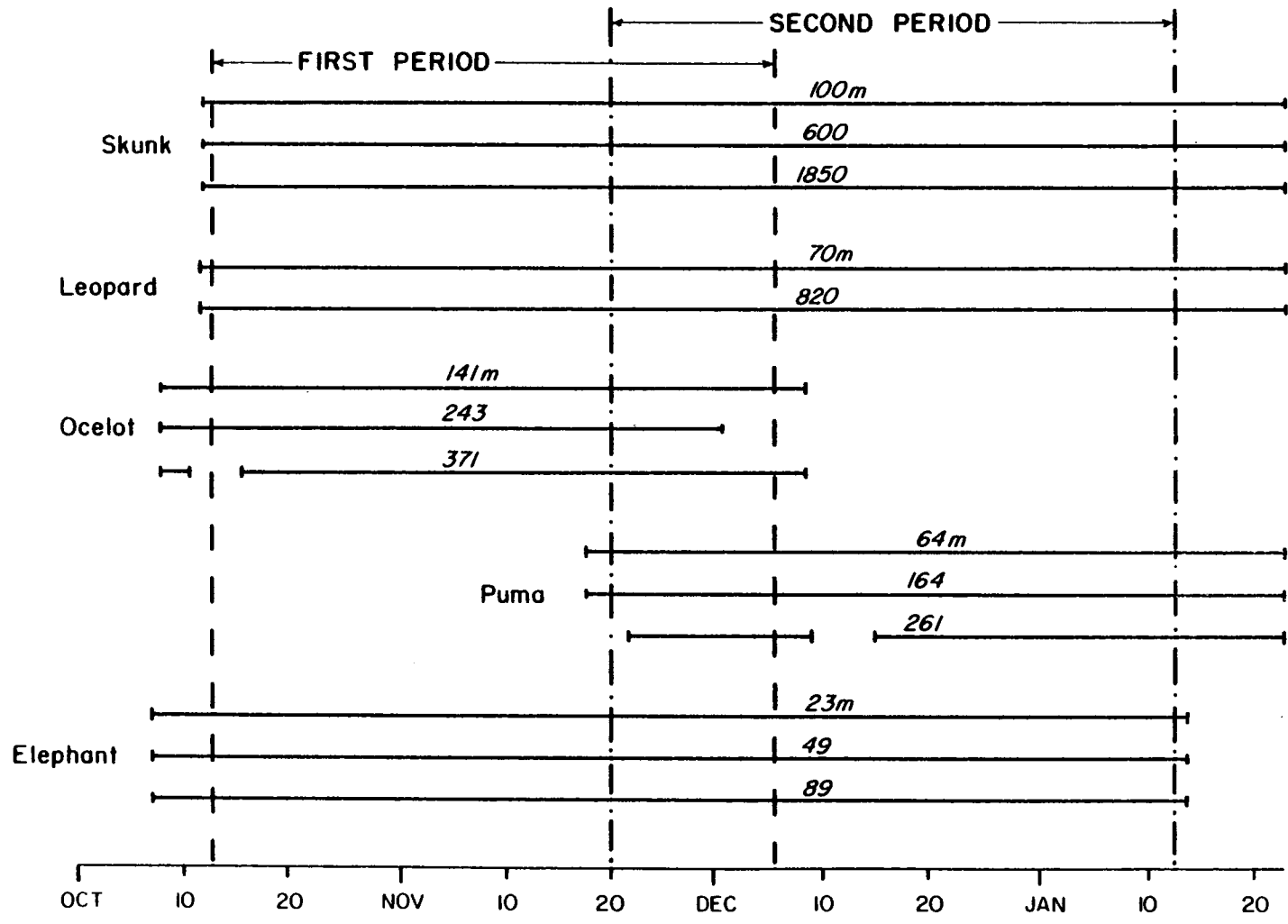


FIGURE 2

with zeroes. The data was filtered with a half power point of 2.5 hours to suppress high frequency signals and then decimated to hourly values to yield the processed data.

The dominance of the near-inertial motion in the processed records is visible in nearly all cases (Figure 3). The long periods of high velocity near-inertial motion will be referred to as "events". Several of these "events" are clearly visible in the Leopard 70m record, particularly the "event" of late October/early November.

Throughout the period of current observations, the wind speed and direction, and the barometric pressure were recorded at Newport, Oregon, about 85 kilometers south of the inshore end of the SUS array.

Hydrographic cruises were conducted occasionally along the moored array by the R/V WECOMA. Several of these cruises were incomplete due to very poor weather conditions (Schramm et al, 1980). Vertical profile of the Brunt-Vaisala frequency, $N^2 = -g/\rho_0 \delta\rho/\delta Z$ (where ρ is density, g is the acceleration due to gravity, and Z is vertically upward), were computed for each cruise using a centered finite difference of 20 meters. Figure 4 shows N^2 profiles for the CTD cast nearest each mooring for three cruises. The N^2 profiles of the casts not shown from each cruise had the same general characteristics as those shown.

During the first cruise (26-29 October), the mixed layer depth was fairly shallow (less than 25m) over the whole array: the only current meter possibly in the mixed layer was Elephant 23m. Skunk 100m, Leopard 70m, Ocelot 141m, and Elephant 49m were located in the pycnocline and the remaining current meters were below the pycnocline.

FIGURE 3

The eastward (U) components of the currents at all eleven current meters of the SUS array. Note the dominance of the near-inertial component in each record.

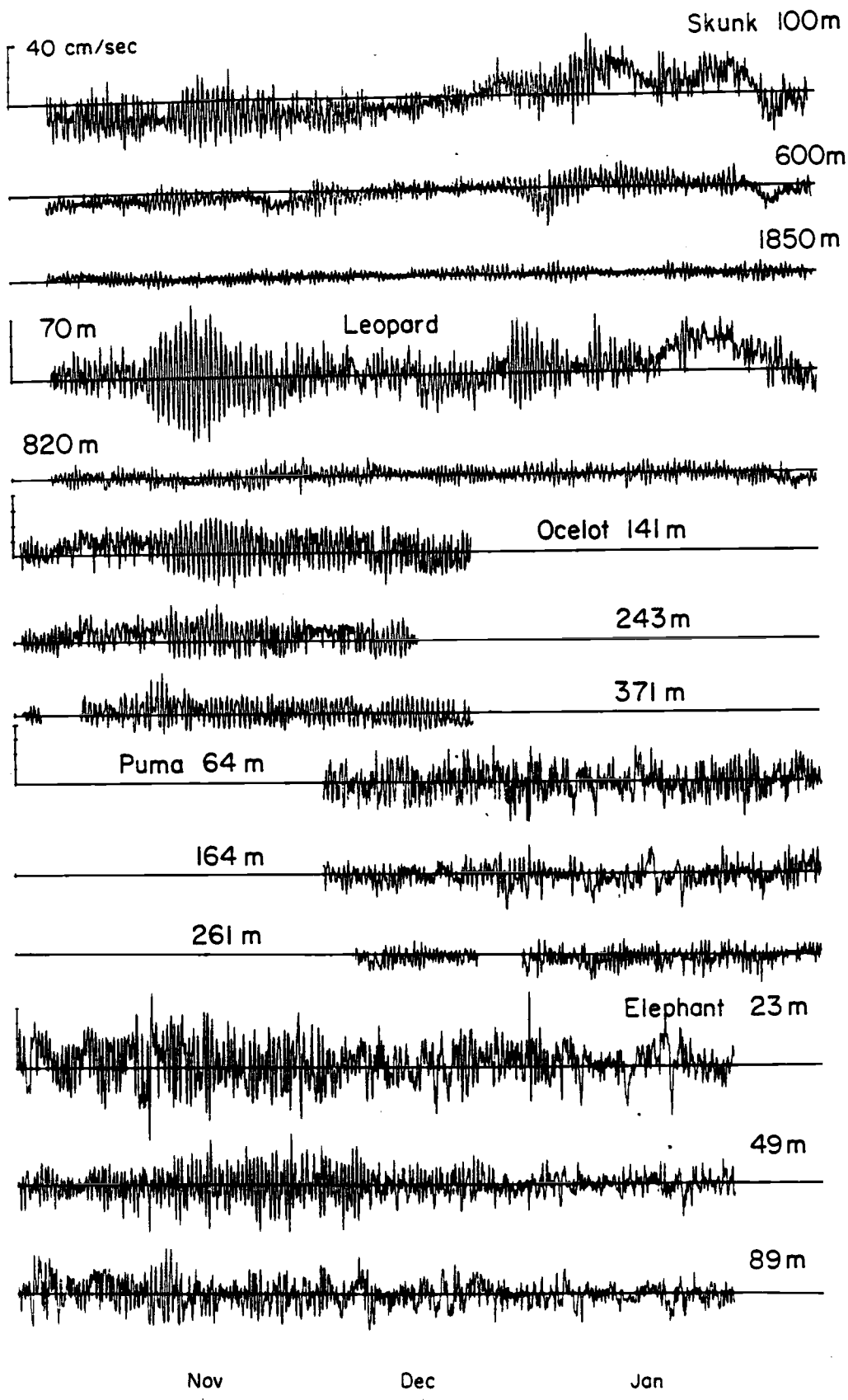


FIGURE 3

FIGURE 4

The Brunt-Vaisala frequency, N^2 , profiles for the CTD cast closest to each current meter on the dates indicated ($N^2 = -g/\rho_0 \Delta\rho/\Delta Z$). A ΔZ of 20 meters was used in the calculations.

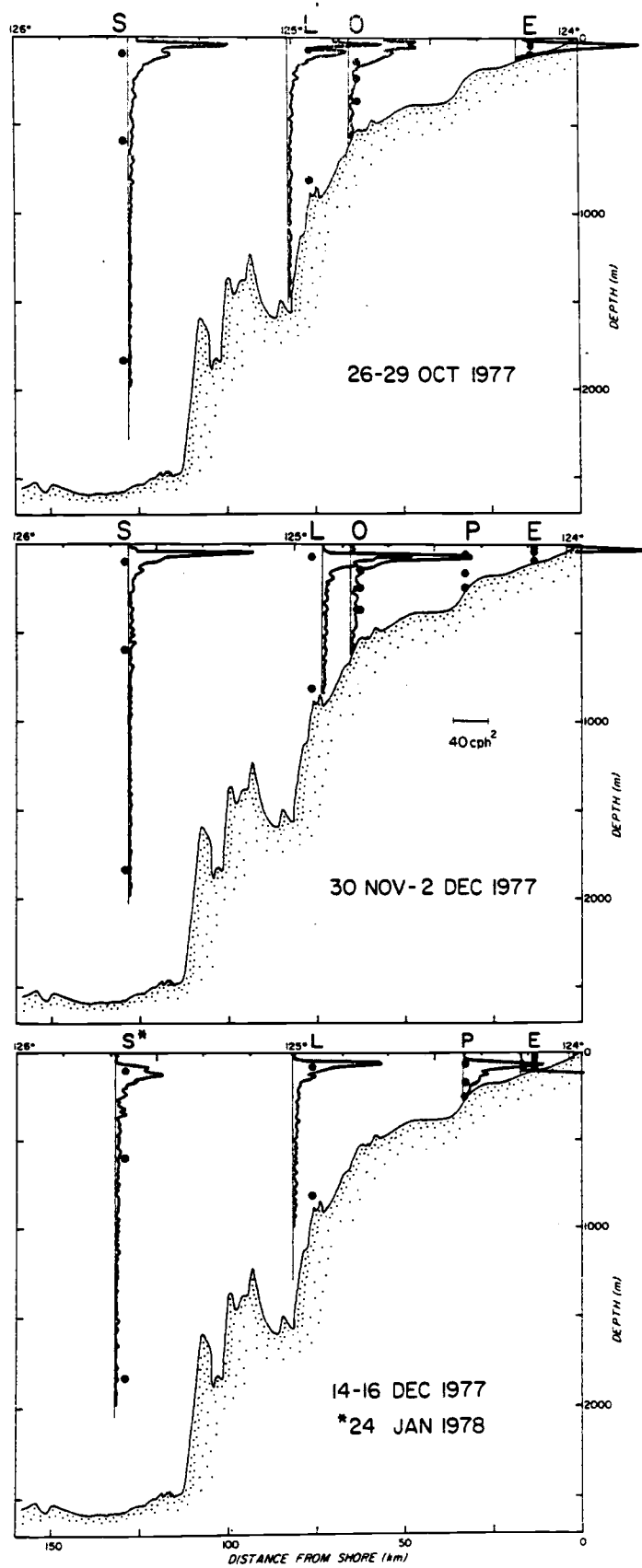


FIGURE 4

During the second cruise, 30 November-2 December, the mixed layer was somewhat deeper, about 40 meters. The location of each current meter with respect to the mixed layer and/or pycnocline was unchanged since the October cruise. Puma had been replaced, but no hydrographic casts were made near it because of bad weather. Puma 64m was probably located in the pycnocline while Puma 164m and 261m were below the pycnocline.

The cast closest to Skunk in the bottom panel of Figure 4 was made on 26 January just before the mooring was removed, while the others were made between 14 and 16 December. The mixed layer at Elephant in December almost reached the bottom placing Elephant 23m and 49m in the mixed layer and 89m in the pycnocline. Ocelot had been recovered prior to the December cruise. The position of the remaining current meters with respect to the pycnocline was unchanged from the previous cruises.

The only two current meters located in the mixed layer for any portion of the observation period were Elephant 23m and 49m. Elephant 23m, with the exception of about 14 days at the beginning of the record, was continuously in the mixed layer. Elephant 49m was in the mixed layer only after mid-December.

SPECTRAL ANALYSIS

Power spectra were calculated for both eastward (U) and northward (V) components of each current meter. The auto and cross-spectra for the U and V components at Leopard 70m (Figure 5) are qualitatively similar to those obtained for the other records. In all cases, there was no significant difference between the amplitude of the auto-spectra of the U and V components at the near-inertial frequencies, and the phase difference was not significantly different from 90° at the 95% significance level (Jenkins and Watts, 1969). Coherence squared (hereafter referred to as coherence) spectra between the U and V components of each current meter were computed for the two time periods described below. At the near-inertial frequencies, U and V were significantly coherent above the 99% level in both time periods at all current meters except Elephant 23m and 49m (Table 1). Since the differences between the U and V auto-spectra were so small and the U and V components were so coherent at the near-inertial frequencies, all further spectral analysis will be confined to just the U component.

Since the common record length for all five moorings was too short (only 390 hours) for meaningful spectral analysis, we used two time periods of 1280 hours which both had simultaneous data from four of the moorings (Figure 2). The first time period, with data from Skunk, Leopard, Ocelot, and Elephant, began at 0400Z 13 October and ended at 1200Z 5 December; this period included the large near-inertial "event" in late October/early November. The second time period started at 0400Z 20 November, ended 1200Z 12 January, and included data from Skunk,

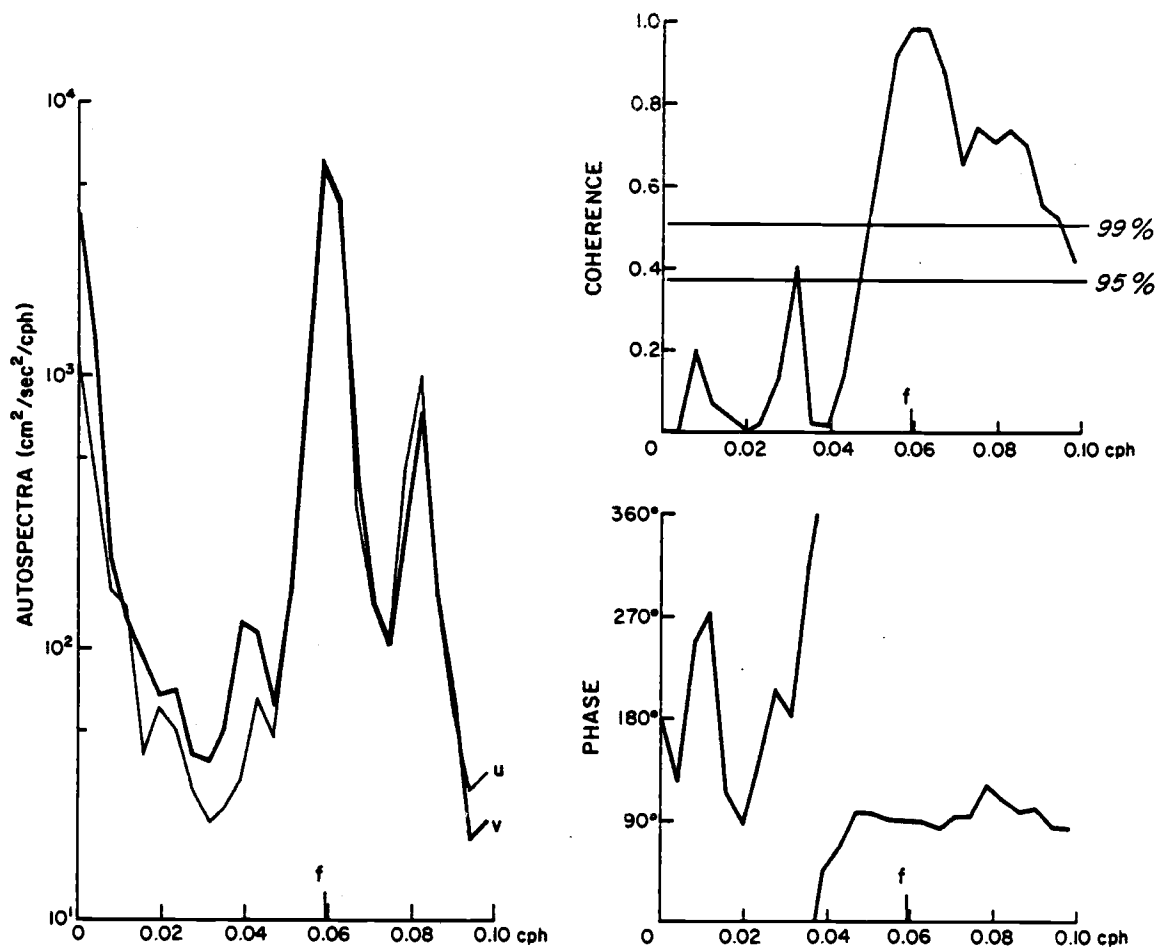


FIGURE 5

The autospectra and cross spectrum of Leopard 70m eastward (U) and northward (V) components for the period 12 October to 5 January. The spectra were computed with 16 degrees of freedom.

TABLE I

Values of coherence squared at the near-inertial frequencies (0.0586 or 0.0625 cph) between U and V components of each current meter.

Values greater than 0.44, 0.53, and 0.68 are significant at the 90% level, 95% level, and 99% level, respectively.

| Current Meter | First Period | Second Period |
|---------------|--------------|---------------|
| Elephant 23m | 0.801 | 0.560 |
| Elephant 49m | 0.929 | 0.495 |
| Elephant 89m | 0.948 | 0.678 |
| Puma 64m | -- | 0.889 |
| Puma 164m | -- | 0.942 |
| Puma 261m | -- | 0.839 |
| Ocelot 141m | 0.981 | -- |
| Ocelot 243m | 0.972 | -- |
| Ocelot 371m | 0.985 | -- |
| Leopard 70m | 0.986 | 0.993 |
| Leopard 820m | 0.990 | 0.967 |
| Skunk 100m | 0.981 | 0.990 |
| Skunk 600m | 0.993 | 0.993 |
| Skunk 1850m | 0.959 | 0.980 |

Leopard, Puma, and Elephant. We allowed the two periods to overlap by 15 days in order to use as much of the available data as possible.

Data gaps due to instrument failure at the beginning of Ocelot 371m and Puma 261m, at the end of Ocelot 243m, and within the Puma 261m records were filled with zeroes. The addition of zeroes reduces the spectral density, but it does not change the basic shape of the resulting power spectra.

Power spectra were computed for each time period by ensemble averaging five spectral periodograms of 256 hour segments. The resulting spectra have ten degrees of freedom, and a bandwidth of 0.0039 cph, 6.5% of f .

The power spectra of the current meters for the four moorings of the first time period (13 October to 5 December) all show prominent peaks at the near-inertial and semi-diurnal frequencies (Figure 6). There is a shift in frequency of the near-inertial peak to a frequency slightly greater than f (by about 1 to 6%) in all cases. This shift in frequency is often observed in the ocean (eg, by Kundu, 1976; Fu, 1981; Gonella, 1971). At eight of the eleven current meters, the near-inertial peak of the power spectrum was greater in magnitude than the semi-diurnal peak. The exceptions were either over the continental shelf (at Elephant 23m and 49m) or in very deep water (Skunk 1850m).

At each mooring, the near-inertial peak was strongest at the shallowest current meter and weakest at the deepest current meter. The amplitude of the near-inertial motion appeared to be relatively constant in the upper 500m. The only current meter that was in the surface layer (Elephant 23m) did not show increased near-inertial energy. This

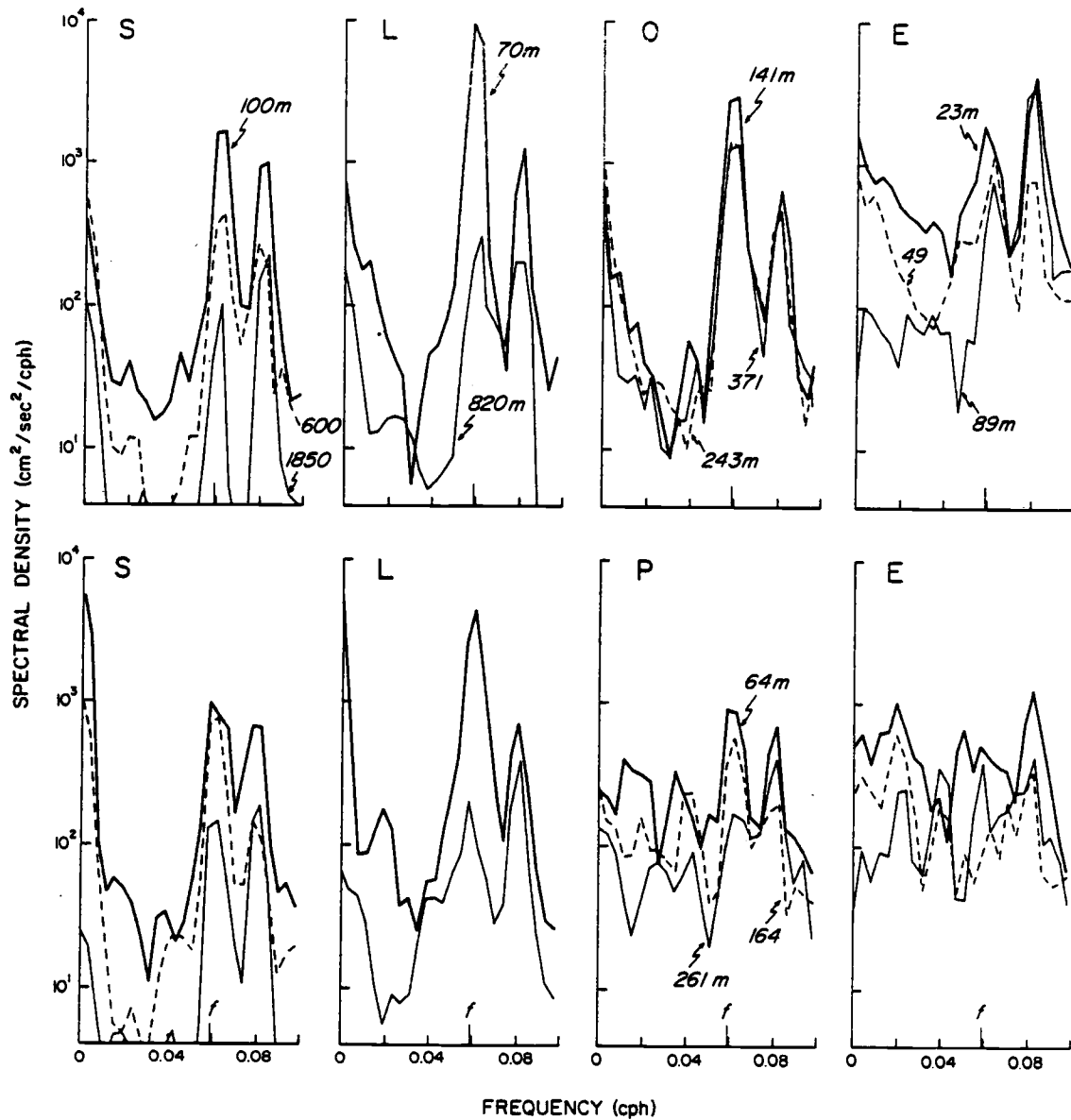


FIGURE 6

The power spectra of the U components for the first period, 13 October to 5 December (upper panel) and second period, 20 November to 12 January (lower panel). S = Skunk; L = Leopard; O = Ocelot; P = Puma; and E = Elephant.

is an apparent contradiction to the observations at Site "D" in the North Atlantic, where near-inertial motions are much stronger in the surface mixed layer than between 50 and 500 meters (Pollard, 1970). However, our only surface-layer observations were over the continental shelf, where dissipation might be higher than offshore. The absence of any offshore current meters shallower than 70m precludes a direct comparison with the depth dependence at Site "D".

During the first period, the average bandwidth of the near-inertial peaks of the eleven records was about 0.007 cph, almost twice the spectral bandwidth of 0.0039 cph. The bandwidth of the peak is defined as the difference between frequencies where the energy falls to one-half of the peak value (Fu, 1981). This peak width is inversely related to the persistence of the near-inertial events (Munk and Phillips, 1968); the average width of 0.007 cph indicates a persistence of about six days.

Power spectra for the second time period show prominent peaks at the near-inertial and semi-diurnal frequencies for the current meters at Skunk, Leopard, and Puma. The shift in frequency of the near-inertial peak for the current meters of these three moorings is similar to that for the first period. The energy contained in the near-inertial frequencies was less than the first time period by about a factor of two. The average bandwidth of the near-inertial peak of all of the current meters for the second time period (0.008 cph) was slightly greater than that for the first time period, implying a persistence of about five days. It is probably not coincidence that the persistence is

less during the less energetic time period. The decrease in energy with depth at the near-inertial frequencies was similar to that for the first time period. There was no apparent correlation between the distance offshore and the amount of near-inertial energy during either time period.

Power spectra for the second time period at Elephant were quite different from the spectra of the other moorings. Both Elephant 49m and 89m show a prominent peak at the diurnal as well as the near-inertial and semi-diurnal frequencies. The near-inertial peak at Elephant 89m is located approximately at f . The power spectra of Elephant 23m and 49m showed two distinct peaks at the near-inertial frequencies. The lesser peak at 23m and the larger peak at 49m showed an upward shift to a frequency several percent above f , similar to the upward shifts at the other moorings. The other near-inertial peak in each of these records showed a downward shift in frequency of about 0.008 cph below f . A weak secondary near-inertial peak at a frequency about 14% below f also occurred at Puma 64m. The three current meters exhibiting a downward frequency shift of the near-inertial peak were all in a region of strong alongshore flow: the average northward current for the second period was about 30 cm/sec at Elephant 23m, 20 cm/sec at Elephant 49m, and 25 cm/sec at Puma 64m. Mean currents can cause a Doppler shift in frequency of the near-inertial peak by the amount:

$$\Delta\omega = k U \cos\gamma$$

where k is the horizontal wave number of the near-inertial motion, U is the magnitude of the mean current, and γ is the angle between the direction of the mean current and the near-inertial motion (Thomson and Huggett, 1981b). Assuming that near-inertial motion with a wavelength of 100 kilometers propagates toward 100°T and that a mean current of 30 cm/sec flowing due north exists, this yields a Doppler shift of -0.012 cph. Hence it seems likely that the downward shift of the near-inertial peak during the second period at Elephant and Puma were due to the strong mean flow there. The current meters which did not exhibit a downward shift in the frequency of the near-inertial peak all experienced relatively weak mean flow.

Coherence spectra among the U components of all current records were computed for both time periods in the same manner as the auto-spectra, i.e., with a bandwidth of 0.0039 cph and ten degrees of freedom. The 90% and 95% significance levels of coherence are 0.44 and 0.53, respectively (Thompson, 1979). The coherence spectrum showed a marked peak at the near-inertial frequencies for most record pairs computed. The larger of the values at either 0.0586 cph (almost equal to f , 0.0592 cph) or 0.0625 cph (5.5% above f) were used to determine whether there was significant coherence between a pair of current meters. The majority of the coherence spectrum peaks occurred above f (at 0.0625 cph) rather than at f .

During the first time period, which included a strong, persistent near-inertial "event" at the beginning of November, many current meter pairs showed significant coherence at the near-inertial frequencies

(Figure 7). Even current meters separated by 115 kilometers (the maximum extent of the moored array) showed coherence well above the 95% significance level (Table 2). In general, there was higher coherence between horizontally separated and diagonally separated pairs than between vertically separated pairs (Figure 7). Only one current meter (Ocelot 37lm) did not show significant coherence with any other current meter. The large lateral coherence scale (> 115 kilometers) indicated by these values exceeds those observed in the open ocean at comparable depths (Fu, 1981) and is comparable to the coherence scales observed in the surface mixed layer at Site "D" in the North Atlantic (Pollard, 1980) and in the relatively shallow waters of Queen Charlotte Sound off British Columbia (Thomson and Huggett, 1981b).

During the second time period, only a few pairs of current meters were significantly coherent at the near-inertial frequencies (Figure 7), even though there was still substantial near-inertial energy at most current meters (Figure 6). The lateral coherence scales during the second time period appeared to vary from less than 20 kilometers between Puma and Elephant to about 50 kilometers between Leopard and Puma. The reduction in coherence scales from the first time period to the second might be associated with the reduction in near-inertial energy (Figure 6) since the radius of the extent of near-inertial motion is directly related to its velocity (Munk and Phillips, 1968). At Elephant there was greater vertical coherence during the second time period than during the first (Figure 7); this may be due to the deepening of the surface mixed layer at Elephant (Figure 4), to nearly include all three

FIGURE 7

The distribution of current meter pairs coherent at the near-inertial frequencies (0.0586 and 0.0625 cph). The pairs connected by solid lines were coherent above the 95% significance level while the pairs connected by the dashed line were coherent above the 90% level.

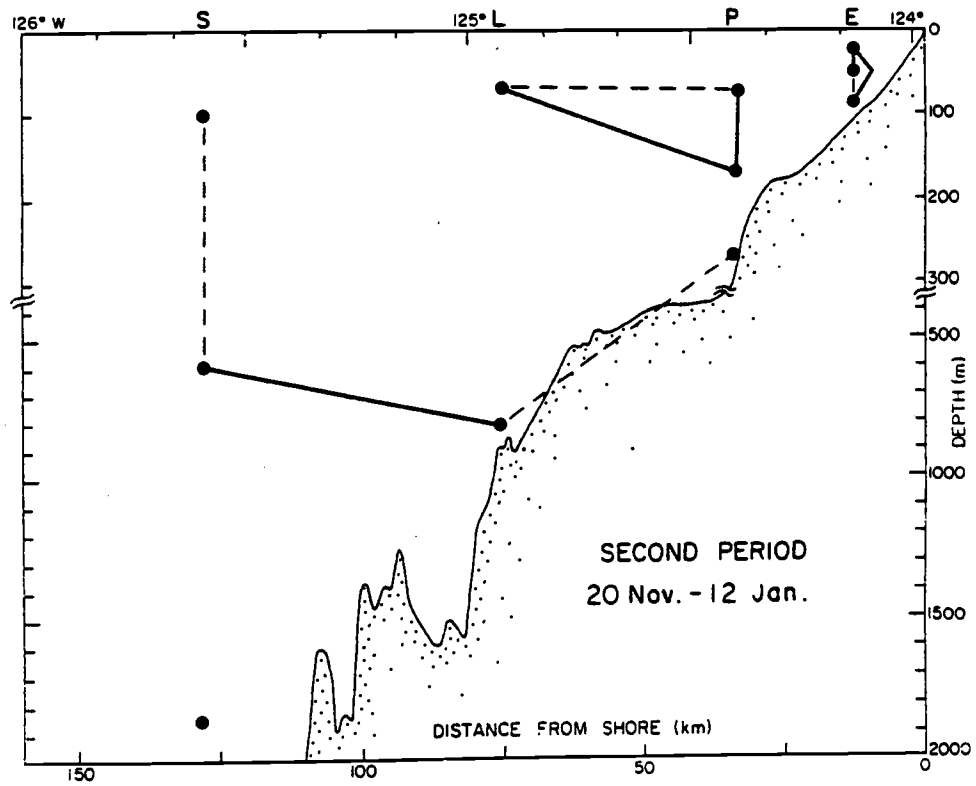
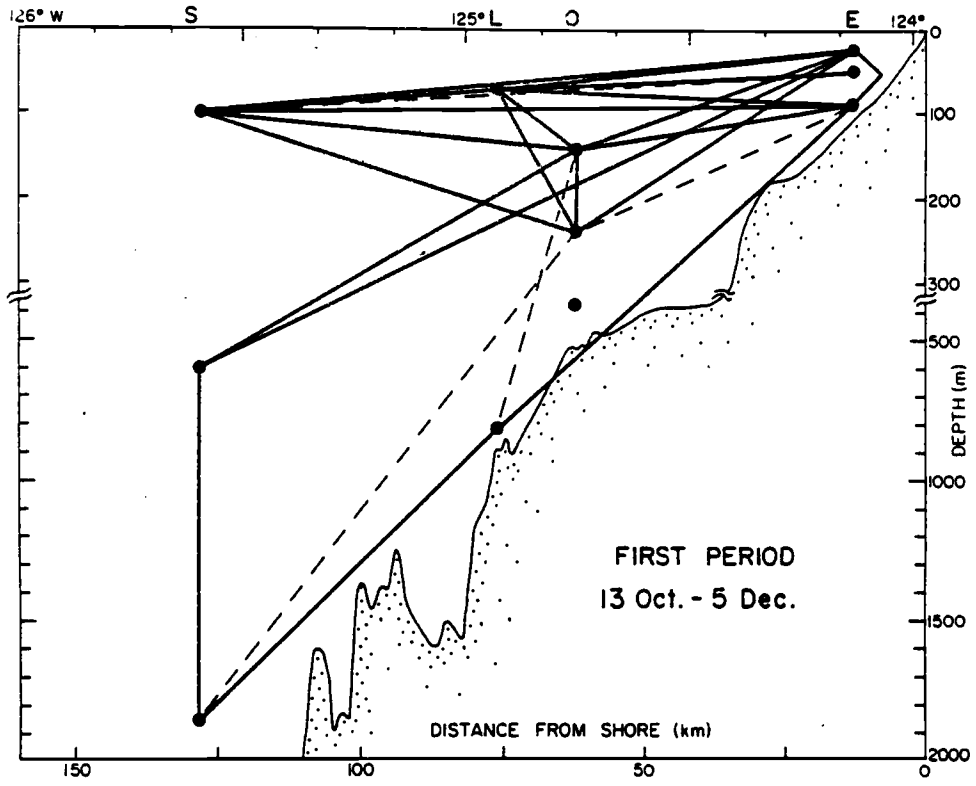


FIGURE 7

TABLE 2

Horizontal east-west (cross-shelf) wavelengths required to account for the phase differences between the nearly horizontally separated current meter pairs.

| Current Meter Pair | Horizontal Separation | Coherence ⁺ | Phase Difference | N | Wavelength* |
|--------------------------------|-----------------------|------------------------|------------------|---|-------------|
| Leopard 70m-Ocelot 141m (71m) | 13.9 km | 0.58 | 100° (± 24°) | 0 | 50 km |
| Ocelot 141m-Elephant 89m (52m) | 48.9 km | 0.67 | 13° (± 20°) | 1 | 47 km |
| Skunk 100m-Leopard 70m (30m) | 52.5 km | 0.56 | 344° (± 25°) | 0 | 55 km |
| Leopard 70m-Elephant 89m (19m) | 62.8 km | 0.57 | 104° (± 24°) | 1 | 48 km |
| Skunk 100m-Ocelot 141m (41m) | 66.4 km | 0.67 | 50° (± 20°) | 1 | 58 km |
| Skunk 100m-Elephant 89m (11m) | 115.3 km | 0.69 | 78° (± 19°) | 2 | 52 km |

⁺ The 90% and 95% levels of significance are 0.44 and 0.53, respectively.

* Horizontal east-west (cross-shelf) wavelength, λ .

$\lambda = \text{separation distance} \times 360^\circ / (\text{Phase difference} + (N \times 360^\circ))$.

N = integral number of 360° added.

current meters. Elsewhere, the stratification remained essentially the same during the second period as it had been during the first time period: all offshore current meters were either in or below the pycnocline.

Phase spectra were also computed for both time periods, but the phase data are meaningful only for the first period when there was generally high coherence among the current meters. The phase data was used to estimate the horizontal east-west (cross-shelf) wavelength of the near-inertial motion of the first time period. We assumed: (1) the vertical separation (maximum of 71m) between Elephant 89m, Ocelot 141m, Leopard 70m, and Skunk 100m was insignificant, i.e., the vertical wavelength was considerably greater than 70m and (2) the horizontal wavelength was larger than the smallest horizontal separation. Phase differences at the near-inertial frequencies among these current meters are shown in Table 2. The smallest horizontal separation between current meters (13.9 kilometers) had a phase difference of $100^\circ (\pm 24^\circ)$ which yields an east-west wavelength of 50 kilometers (the 95% confidence interval is 40 to 66 kilometers). By adding integral numbers of 360° to the phase differences between the other pairs of current meters, we were able to obtain consistent estimates of the cross-shelf wavelength (Table 2). All of the values obtained were well within the 95% confidence limits of the estimate based only on the Leopard 70m-Ocelot 141m phase difference. The 50 kilometer horizontal wavelength obtained for the first period is consistent with the large horizontal coherence scales during the period (a little over two wavelengths spans the entire array).

We also considered estimating the vertical wavelength, but there was significant coherence between only a few vertically separated current meters. The spacing between the current meters was also too large to resolve vertical wavelengths of the magnitude (50 to 500 meters) usually observed in the ocean.

BAND-PASSED DATA

In order to examine the time variability of the near-inertial motion, we band-passed the records using a narrow filter centered at 0.0625 cph, the most common frequency of the near-inertial peak in the autospectra. The center component of the filter, where 100% of the energy was passed, was 0.025 cph wide. The edges of the filter tapered linearly to zero over a width of 0.002 cph (Figure 8). The narrow width of the filter was required because of the close proximity of the tidal frequencies to f . The band-pass filter program used a Sande-Tukey fast Fourier transform and set the Fourier components outside the filter frequencies to zero. The remaining components were transformed back to the time domain to yield the band-passed data.

The possibility of peak smearing due to the sharp filtering was tested using a synthetic 1024 hour series with 5, 10, or 15 cycles of motion at 0.0625 cph. The remainder of the series was set to zero. The results of applying the band-pass filter to the synthetic time series shows peak smearing is less pronounced when the number of cycles was greater. When the input series contained more than 10 cycles, the amplitude of the band-passed output did not vary greatly from the input series. The more energetic near-inertial "events" in our data consisted of ten or more cycles (Figure 3). It is felt the amplitude of the band-passed output is representative of the actual near-inertial motion amplitude for these "events". The phase of the near-inertial motion, regardless of the number of cycles, was not altered by the band-pass filter.

FIGURE 8

The response curve of the band passed-filter (upper left panel), and examples of band-passed (dashed) time series of synthetic input series (solid) of 5, 10, and 15 cycles at 0.0625. Total length of the synthetic time series was 1024 hours.

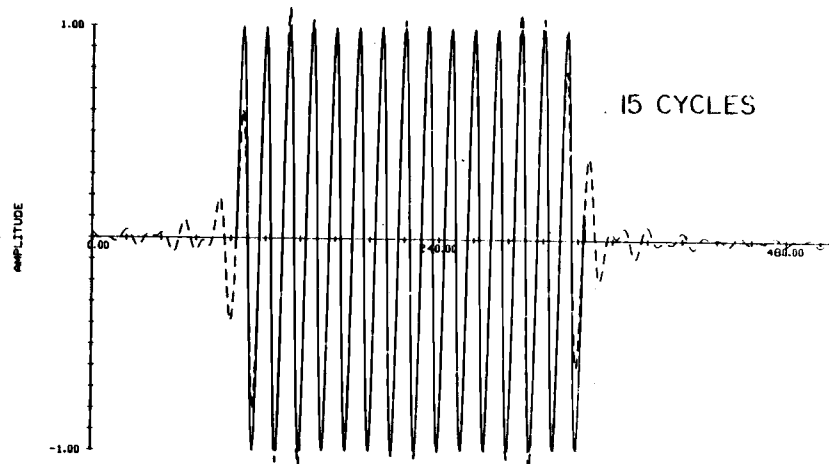
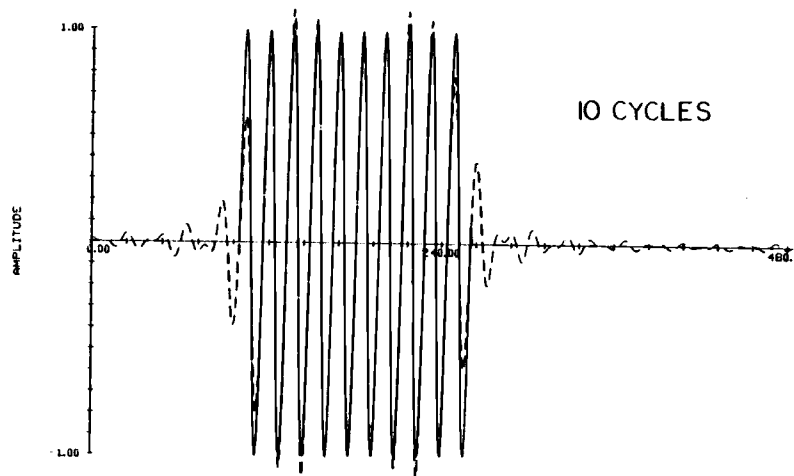
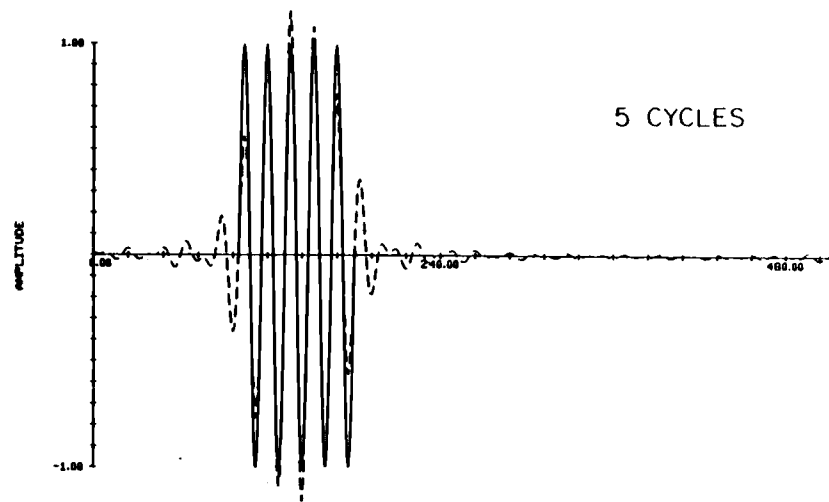
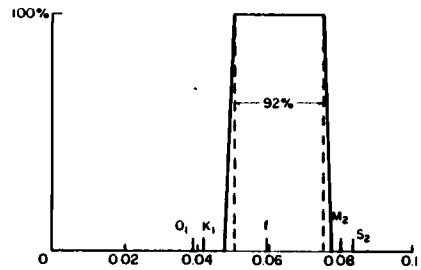


FIGURE 8

The band-passed U component of each record is shown in Figure 9. The length of each band-passed record was 2048 hours except at Ocelot (1408 hours) and Puma (1280 hours). Note the presence of near-inertial motion throughout the entire length of all the band-passed records except possibly Skunk 1850m, Leopard 820m, and Puma 261m. The maximum value of the band-passed data (41.1 cm/sec) occurred at Leopard 70m during the "event" in late October/early November, which is visible in the band-passed records of the three offshore moorings. The dominance of the near-inertial component in both the U and V components of Leopard 70m is clearly visible in Figure 10. Note the extreme similarity of the U and V band-passed components. An expanded section of the Leopard 70m U and V components shows clearly the approximate 90° lag of U behind V (Figure 11).

During each period of high near-inertial energy, the phase differences between the band-passed records of Skunk 100m, Leopard 70m, and Ocelot 141m remained constant. The phase differences between the band-passed records of Skunk 100m, Leopard 70m, and Ocelot 141m for the "event" in late October/early November were the same as the spectral phase differences obtained for the first period, i.e., the wavelength during that "event" is probably 50 kilometers, as estimated in the previous section. During 18-22 December, however, the phase difference between Leopard 70m and Skunk 100m was 90°; implying an east-west horizontal wavelength of about only 40 kilometers. Thus, the wavelength of the near-inertial motion appears to be well defined and constant during a particular "event", but may vary between different "events".

FIGURE 9

The eastward (U) components of the band-passed time series for all eleven current meters of the SUS array. Note the presence of near-inertial "events" in most records.

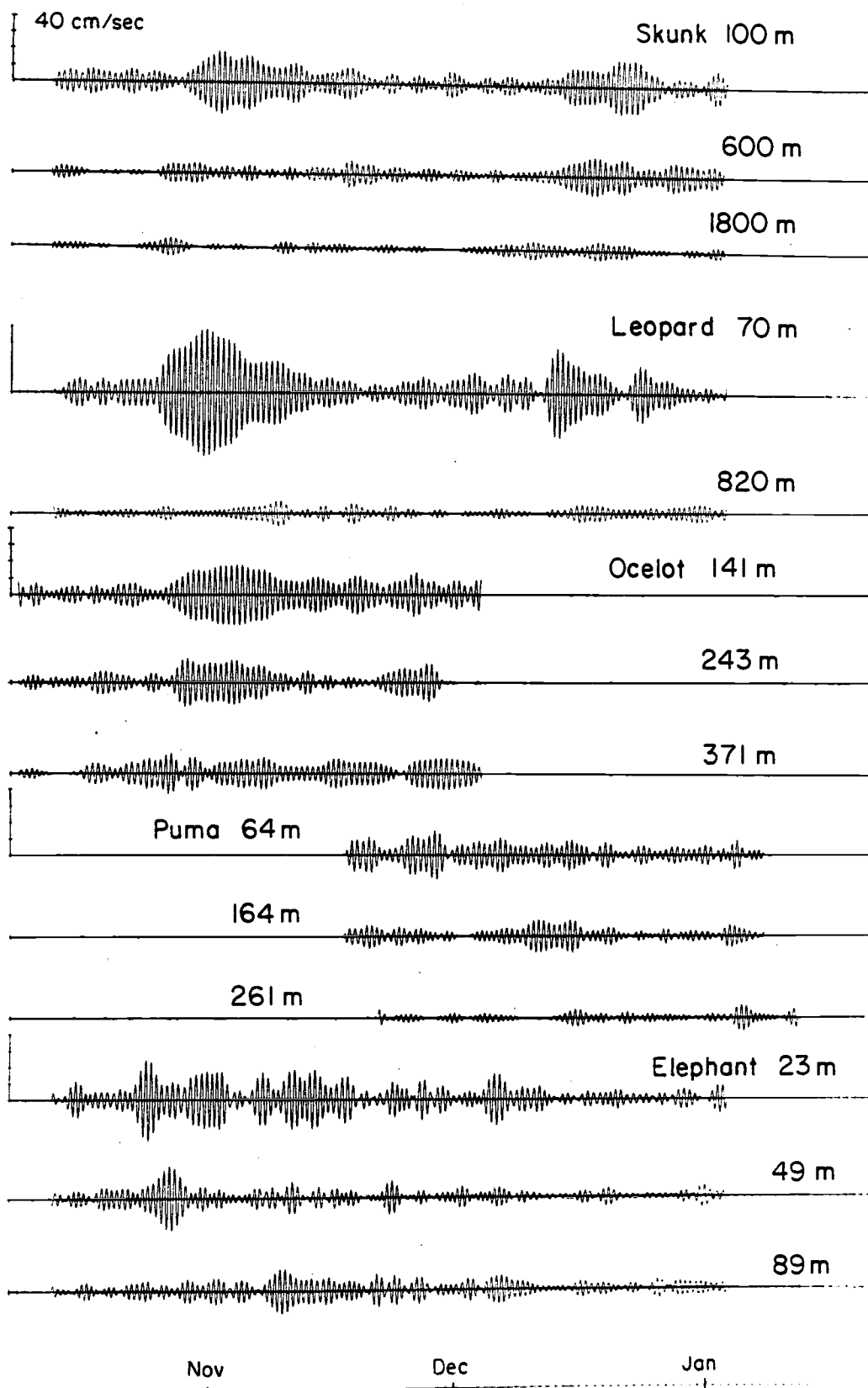
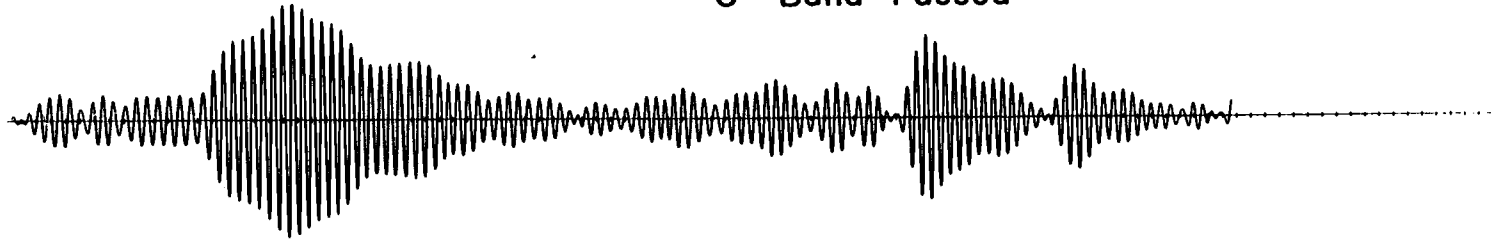


FIGURE 9

FIGURE 10

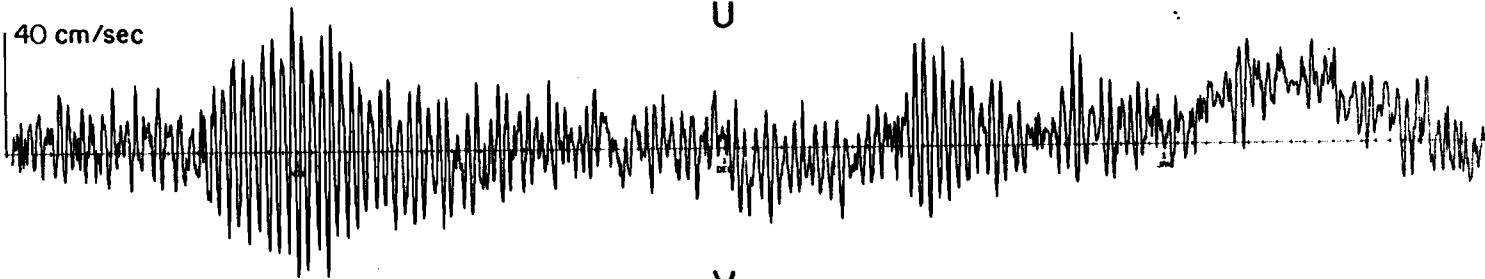
The U and V components of the processed and band-passed records of Leopard 70m. Note the similarity between the components and the dominance of the near-inertial component of the processed records.

U Band Passed

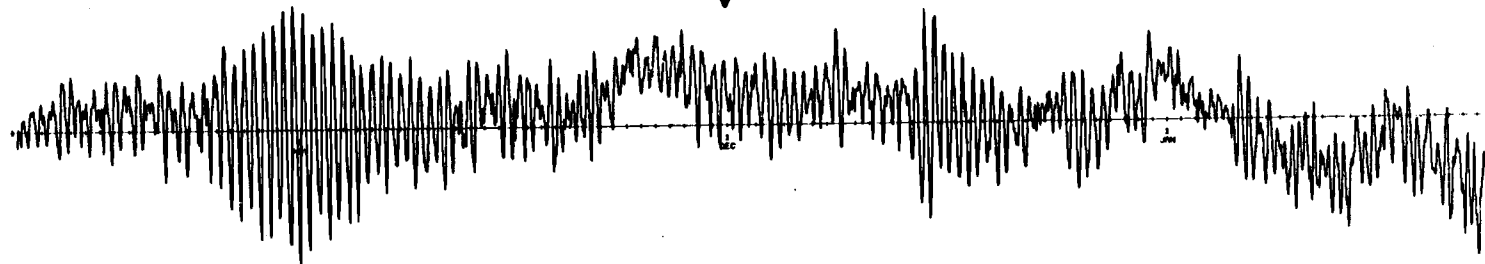


40 cm/sec

U



V



V Band Passed

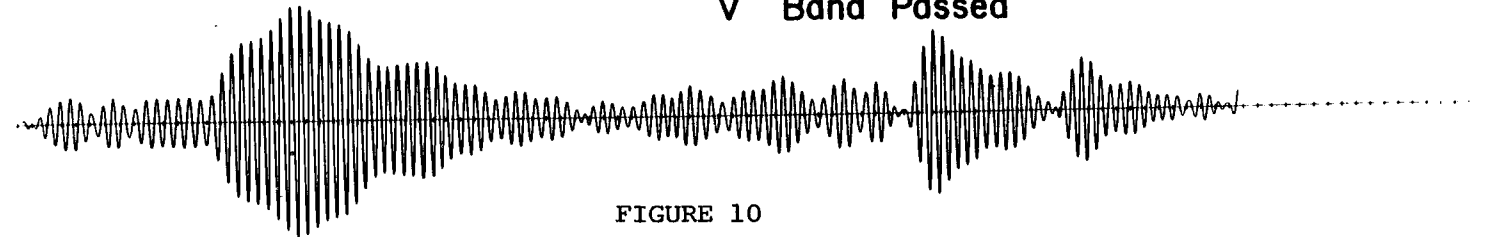


FIGURE 10

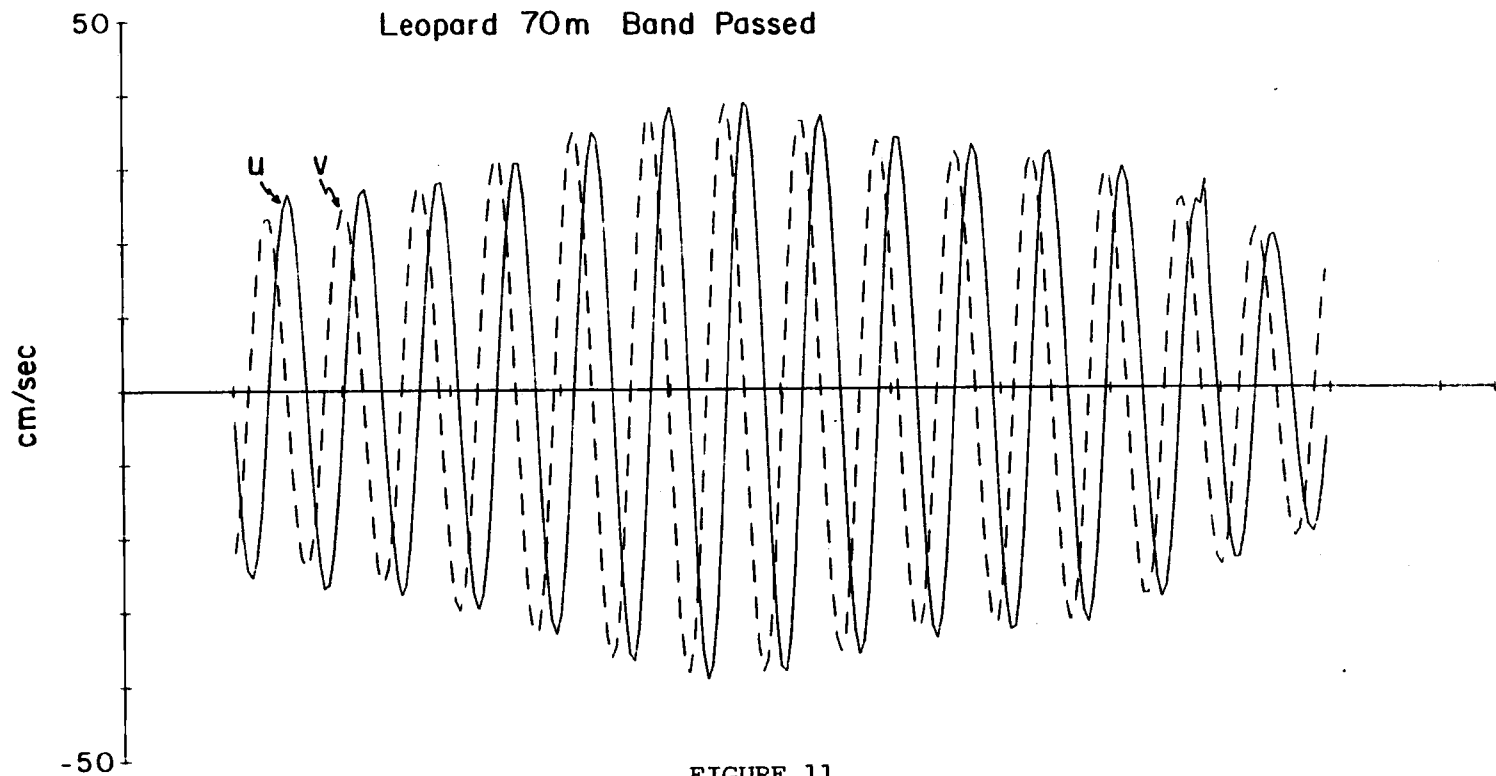


FIGURE 11

A ten day (27 October to 6 November) expanded section of the band-passed U and V components of Leopard 70m from the "event" of late October/early November. Note the approximate 90° lag of U behind V.

WIND FORCING

We wanted to estimate qualitatively the near-inertial motions which could have been generated in the mixed layer by the surface winds. Pollard and Millard (1970) found a good correlation between observed near-inertial motions in the mixed layer at Site "D" in the North Atlantic and a computed current based on a simple model of wind forcing. We applied the Pollard and Millard model using wind data recorded at Newport as the forcing function. The model equations are:

$$\partial U / \partial t - fV = \tau_x / (\rho Z) - cU \quad (1)$$

$$\partial V / \partial t + fU = \tau_y / (\rho Z) - cV \quad (2)$$

where f is the local inertial frequency, c^{-1} is the e-folding time scale of the motion (c is the damping coefficient), ρ is the water density (1 gm/cm^3) and $\tau(\tau_x, \tau_y)$ is the wind stress. The wind stress was computed by:

$$\vec{\tau} = C_d \rho_a |\vec{V}| \vec{V} \quad (3)$$

where \vec{V} is the hourly wind. The density of air (ρ_a) was set at $1.25 \times 10^{-3} \text{ gm/cm}^3$ and the drag coefficient (C_d) was set at 1.5×10^{-3} . We assumed a constant mixed layer depth, Z , of 25 meters.

Rewriting (1) and (2) in finite difference form we get:

$$(U_2 - U_1) / \Delta t = fV_1 + \tau_x / (\rho Z) - cU_1 \quad (4)$$

$$(V_2 - V_1) / \Delta t = -fU_1 + \tau_y / (\rho Z) - cV_1 \quad (5)$$

If we assume the forcing functions, τ_x and τ_y , and the damping factor, c , are zero, then (4) and (5) can be written as:

$$U_2 = U_1 + fV_1 \Delta t \quad (6)$$

$$V_2 = V_1 + fU_1 \Delta t \quad (7)$$

If an initial velocity (energy) is given to the system, the equations of the model as written in (6) and (7) should result in a current vector of the initial given magnitude rotating with a period of $1/f$; i.e., energy should be conserved. However, the energy at time 2 is given by:

$$\begin{aligned} U_2^2 + V_2^2 &= (U_1 + fV_1 \Delta t)^2 + (V_1 - fU_1 \Delta t)^2 \\ &= (U_1^2 + V_1^2) (1 + (f\Delta t)^2) \end{aligned} \quad (8)$$

As can be seen from (8), energy on the order of $(f\Delta t)^2$ has been "added" to the system. We tested different values of Δt to determine which value would not significantly alter the energy in the system and found that Δt had to be four seconds or less to achieve this goal. Therefore, a four second time step was used to compute the model current. Hourly values were retained for output of the model current.

The Pollard and Millard model shows a strong near-inertial response to the wind stress peaks of mid-December and early January (Figure 12). The model results were compared to the observed near-inertial motions of a current record in the mixed layer (Elephant 23m) and another about 30 meters below the mixed layer (Leopard 70m). There is qualitative agreement between the U component of the model current and the band-passed record of Elephant 23m for the periods 22-26 October, 3-18 November and 6-10 December, but Elephant 23m does not show a response to the wind stress peaks of mid-December and early January. Leopard 70m however does show a marked response to the wind stress peak in mid-December and a weaker response to the one on 4 January.

FIGURE 12

The magnitude of the Newport wind stress, and the U components of the Pollard and Millard model and Elephant 23m (in the mixed layer) and the Leopard 70m (about 30m below the mixed layer) band-passed records. The Pollard and Millard model was generated using the Newport wind stress as the forcing function.

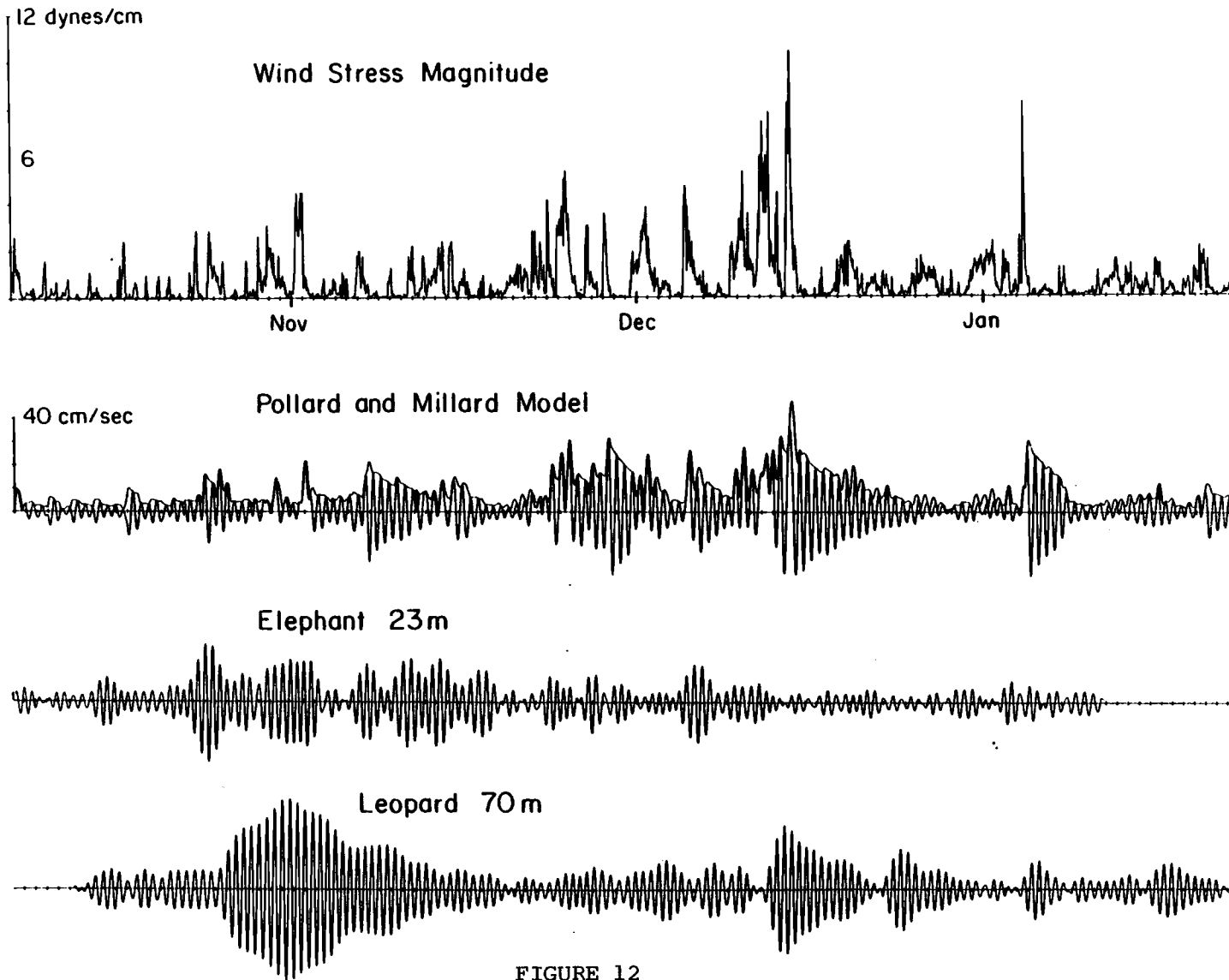


FIGURE 12

The wind used to model the surface currents for the SUS array was measured on the beach about 100 kilometers from the array center. The actual wind over each mooring of the array was probably somewhat different than that recorded at Newport. Pollard (1980) found through comparison of modeled currents using wind observations separated by about 50 kilometers at Site "D" that the Pollard and Millard model is very sensitive to small variations in the wind field. In spite of this, the model current using the Newport wind seems to account for the gross response of Leopard 70m to the large peaks in the wind stress even though Leopard 70m was well below the mixed layer.

The model current failed to account for the long, energetic "event" of late October/early November. Since the model is sensitive to small-scale variations in the wind field, we might expect poor agreement between observed currents and model results based on the (relatively distant) Newport winds whenever there are strong atmospheric fronts in the region. As well as reflecting inhomogeneities in the wind field, a frontal passage is generally associated with a brief clockwise rotation of the wind direction, which is particularly effective in generating near-inertial motions (Pollard, 1980; Thomson and Huggett, 1981b). Fluctuations in the wind field of a period less than an inertial period (such as those associated with fronts) are most effective in generating or destroying near-inertial motions by the process of constructive/destructive interference (Pollard, 1970).

Synoptic atmospheric surface pressure charts showed frequent strong fronts in the area during late October and early November: examples are

shown in Figure 13. Between October 23 and November 15, seventeen fronts associated with low pressure centers of varying size and intensity passed west to east over the SUS array. The hourly barometric pressure record from Newport (Figure 13) was used to check some of the approximate frontal passage times estimated from the synoptic charts. Clockwise fluctuations of the wind direction associated with frontal passages are evident in the direction of the low-passed (< 0.025 cph) wind at Newport during this period (Figure 13). Since the extent of the SUS array was 115 kilometers, the arrival time of each front would not generally be the same time at all moorings. If the rotation of the near-inertial motion caused by each frontal passage was in phase with the existing near-inertial motion, a long, energetic "event" would be formed. No phase shifts were observed at Leopard 70m during late October/early November, while several phase shifts were observed at Elephant 23m during the same period (Figure 14). Apparently all of the wind generated near-inertial motion near Leopard in late October/early November was in phase, thus creating the large "event" observed there. On the other hand, some of the near-inertial motion near Elephant was probably out of phase with pre-existing near-inertial motions, causing destructive interference on about 27 October and again on 4 and 6 November. Following 15 November, there was a seven day period in which no fronts passed over the SUS array apparently allowing the energy of the "event" at Leopard 70m, and elsewhere in the array, to dissipate. Without direct wind observations over the moorings, these tentative conclusions cannot be verified.

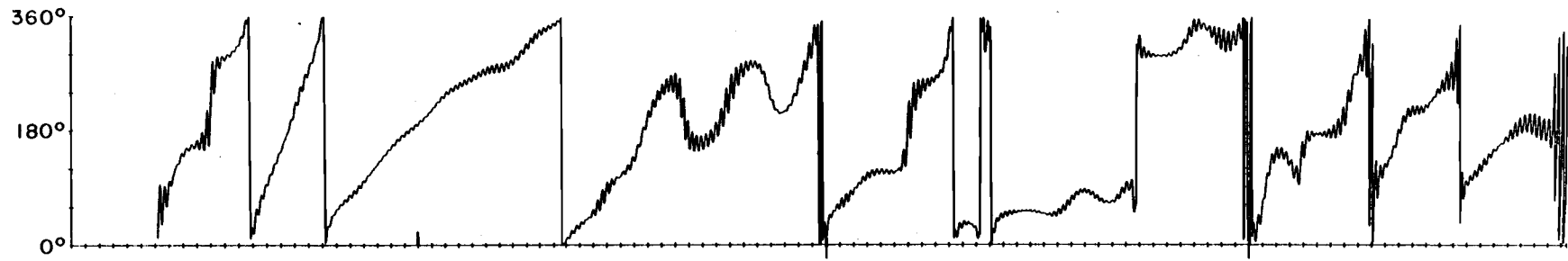
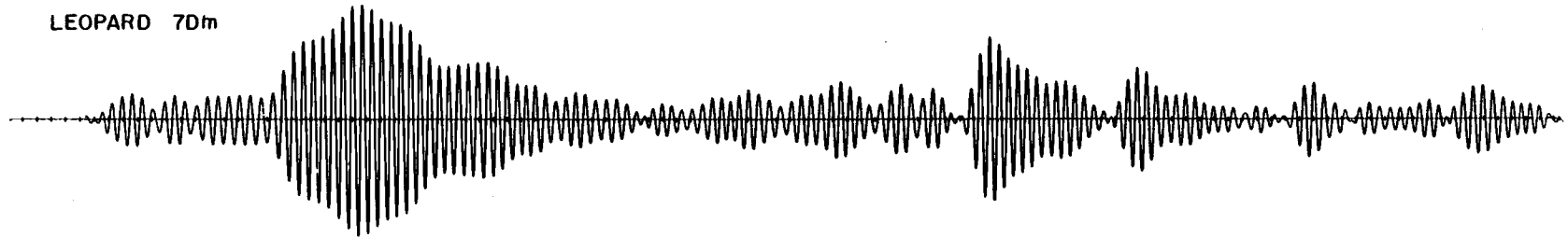
FIGURE 13

The direction of the low-passed (< 0.025 cph) Newport wind, the Newport barometric pressure, and examples of the surface synoptic charts from the period of the near-inertial "event" of late October/early November.

FIGURE 14

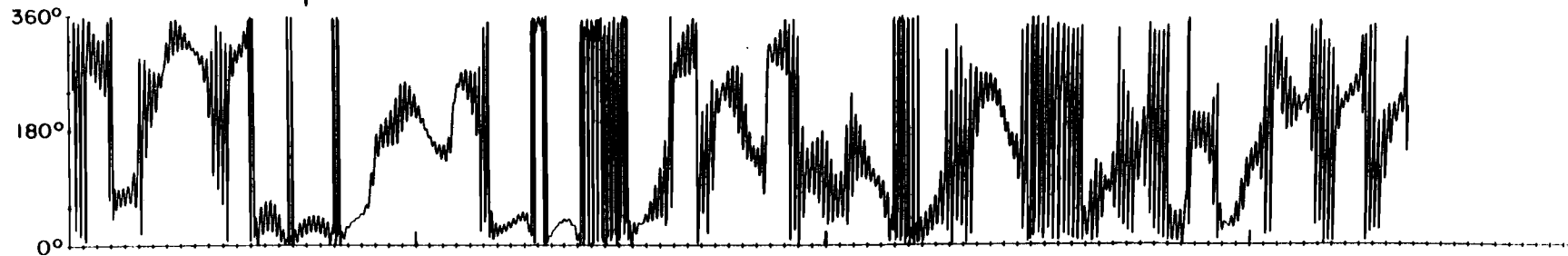
Time series of the difference in phase between the Leopard 70m and Elephant 23m band-pass current vectors and a reference vector rotating with a frequency of 0.0625 cph. A linear slope indicates a constant phase for the near-inertial motion of the band-passed records.

LEOPARD 70m



LEOPARD 70m Phase Difference

ELEPHANT 23m



ELEPHANT 23m Phase Difference

Nov

Dec

Jan

FIGURE 14

SUMMARY

The observed near-inertial motions of the SUS array were below the mixed layer except those from Elephant 23m and the end of the Elephant 49m record. Near-inertial motions observed were present almost continuously in all eleven current records. The maximum near-inertial velocity (41 cm/sec) was greater than the expected norm of 20-30 cm/sec, particularly considering it occurred at a depth of 70 meters, well below the mixed layer.

For spectral analysis, the total observation time was divided into two overlapping time periods with the first containing the "event" of late October/early November. The autospectra generally showed an upward shift in frequency of several percent of ω above f . The autospectra of Elephant 23m and 49m, and Puma 64m for the second time period showed the near-inertial peak about 14% below f . The downward shift in frequency of ω below f for these cases can be accounted for by a Doppler shift associated with the strong mean flow in the upper water column over the shelf.

The scales of coherence for the two time periods selected were quite different. The coherence scales observed for the second time period were of the same order as those described in the introduction (tens of kilometers horizontally and tens of meters vertically) as common. The high diagonal coherence values observed in the first time period have not been observed before: pairs of current meters separated diagonally (up to 115 kilometers horizontally and 500 meters vertically) were significantly coherent above the 95% level. An east-west (cross-shelf) wavelength of about 50 kilometers was determined for the first

period from the phase differences between current meter pairs with roughly horizontal separations. This long wavelength helps account for the large horizontal part of the diagonal coherence scale.

The numerous fronts associated with low pressure centers appeared to be the primary generation mechanism of the large near-inertial "event" of late October/early November observed at Leopard 70m, even though the current meter was about 30 meters below the mixed layer. All of the energy arriving at Leopard 70m during the "event" was in phase. The similarity of responses of Leopard 70m and the Pollard and Millard model to peaks in the wind stress in mid-December and early January indicate surface winds can be responsible for near-inertial motions observed below the mixed layer.

We conclude surface wind events can be the primary generation mechanism for near-inertial motions observed below the mixed layer. The phase of the energy added by succeeding wind events, especially fronts, determines the magnitude of the near-inertial motions that can be formed both in and below the mixed layer. The horizontal coherence scales of near-inertial motions below the mixed layer can be much greater than those previously accepted as common in the literature.

BIBLIOGRAPHY

- Barstow, D.A., W. E. Gilbert, R.E. Schramm, B.M. Hickey, A. Huyer, and R. L. Smith. (1979). Moored Current Meter Observations from the Slope Undercurrent Study off Oregon, July 1977-October 1978. Unpublished data report.
- Fu, L. (1981). Observations and models of Inertial Waves in the Deep Ocean. Review of Geophysics and Space Physics, 19, 141-170.
- Gonella, J. (1971). A Local study of inertial oscillations in the upper layers of the ocean. Deep Sea Research, 18, 775-788.
- Jenkins, G.M. and D.G. Watts. (1969). Spectral Analysis and Its Applications. San Francisco, Holden-Day, 525 pp.
- Johnson, W. (1976). Cyclesonde Measurements in the Upwelling Region off Oregon. Rosential School of Marine and Atmospheric Sciences, University of Miami Technical Report 76-1, 124 pp.
- Kindle, J. C. (1974). The horizontal coherence of Inertial Oscillations in a Coastal Region. Geophysical Research Letters, 1, 127-130.
- Kroll, J. (1975). The propagation of wind generated inertial oscillations from the surface into the deep ocean. Journal of Marine Research, 33, 15-51.
- Kundu, P.K. (1976). An analysis of inertial oscillations observed near the Oregon Coast. Journal of Physical Oceanography, 6, 879-898.
- Munk, W., and N. Phillips. (1968). Coherence and band structure of inertial motion in the sea. Review of Geophysics, 6, 447-471.
- Pollard, R.T. (1970). On the generation by winds of inertial waves in the ocean. Deep Sea Research, 17, 795-812.
- Pollard, R.T. (1980). Properties of near-surface inertial oscillations. Journal of Physical Oceanography, 10, 385-398.
- Pollard, R.T. and R.C. Millard. (1970). Comparison between observed and simulated inertial oscillations. Deep Sea Research, 17, 815-821.
- Schramm, R.E., D.A. Barstow, W.E. Gilbert, and A. Huyer. (1980). CTD observations from the Slope Undercurrent Study off Oregon, July 1977-October 1978. Unpublished preliminary data report.
- Thompson, R.O.R.Y. (1979). Coherence Significance Levels. Journal of Atmospheric Sciences, 10, 2020-2021.

- Thomson, R.E. and W.S. Huggett. (1981a). Wind-driven inertial oscillations within Queen Charlotte Sound and Hecate Strait, May-September 1977. Pacific Marine Science Report 81-20, Institute of Ocean Sciences, Sidney, B.C., 90 pp.
- Thomson, R.E. and W.E. Huggett. (1981b). Wind driven Inertial Oscillations of large spatial coherence. Atmosphere-Ocean, 19, 291-306.
- Webster, F. (1968). Observations of inertial-period motions in the deep sea. Review of Geophysics, 6, 473-490.